REPORT

APPLIED PHYSICS

Wrapping with a splash: High-speed encapsulation with ultrathin sheets

Deepak Kumar,^{1,2} Joseph D. Paulsen,³ Thomas P. Russell,^{2,4,5,6} Narayanan Menon¹*

Many complex fluids rely on surfactants to contain, protect, or isolate liquid drops in an immiscible continuous phase. Thin elastic sheets can wrap liquid drops in a spontaneous process driven by capillary forces. For encapsulation by sheets to be practically viable, a rapid, continuous, and scalable process is essential. We exploit the fast dynamics of droplet impact to achieve wrapping of oil droplets by ultrathin polymer films in a water phase. Despite the violence of splashing events, the process robustly yields wrappings that are optimally shaped to maximize the enclosed fluid volume and have near-perfect seams. We achieve wrappings of targeted three-dimensional (3D) shapes by tailoring the 2D boundary of the films and show the generality of the technique by producing both oil-in-water and water-in-oil wrappings.

any liquid-phase technologies require the encapsulation of one liquid in another. In the stabilization of emulsions, drug delivery, and remediation of oil spills, liquid droplets are separated from the surrounding liquid by a fluid monolayer of molecular or particulate surfactants (1-3). By contrast, we typically wrap solid contents, such as chocolates or the filling in a dumpling, with solid elastic sheets. Solid wrappings of liquids would allow new possibilities, such as drops with nonspherical shapes, designed permeability, and mechanical shear rigidity. Sufficiently thin planar sheets will spontaneously wrap liquid droplets by balancing the elastic energy of curving the sheet with the reduction in interfacial surface energies. Elastomer films of thickness $t \sim 100 \, \mu \text{m}$ were shown to bend around a water droplet by this mechanism (4, 5). For much thinner films, the energetic cost of bending becomes negligible compared with the surface energies (6). Paulsen et al. (7) found that in this regime of highly bendable sheets (8), the wrappings are optimal in the sense that they enclose the maximum volume within a fixed area of sheet. However, those experiments changed the volume of the liquid quasistatically and required controlled initial conditions that are not scalable for the rapid production of wrapped drops.

Here, we establish a fast, dynamic route to wrapping in the high-bendability regime, exploiting the dynamics generated by the impact of a drop of oil on an ultrathin polymer sheet floating on a pool of water. Polystyrene films of thickness t from 46 to 372 nm are cut into circular discs of radius W = 1.6 to 3.2 mm and placed on the water surface in a cuvette (9) as shown in Fig. 1. A drop of fluorinated oil of radius R = 0.6 to 1.2 mm, density ρ_{oil} = 1800 kg/m³, and surface tension γ_{oil} = 16 mN/m is released from a height h = 10 to 300 mm above the surface. The drop hits the surface with a kinetic energy proportional to h. Immediately after the impact, a crater begins to form, which reaches a maximum depth and then retracts back toward a flat interface. During the retraction, the drop separates from the water-air interface while the sheet wraps around the drop. Despite the uncontrolled dynamics of the splash, the drop achieves optimal wrapping, both in terms of the three-dimensional (3D) shape of the wrapped drop (7) and in the near-perfect closure achieved along the seam. This sequence of events takes tens of milliseconds to complete (movie S1). Once the wrapped oil separates from the water surface, it sinks under gravity.

The static 3D shape is optimal when the exposed area of the fluid interface is minimized, as in Eq. 1 (7)

$$U = \gamma A_{free}$$
 (1)

where the only dimensionless control parameter is W/R, the ratio of the sheet radius to the droplet radius. In the dynamical splashing process, the energies of the initial and final state involve the surface energy of the partially or fully wrapped drop, as well as the energies of all other interfaces between the air, oil, water, and sheet. The final energy is higher, which implies that an energy barrier (9) must be overcome by the kinetic energy of the drop. As is typically done in splashing problems (10), we take the ratio of the kinetic energy at impact to the initial surface energy of the drop to form the dimensionless

Weber number, $We=rac{
ho_{oll}v^2R}{\gamma_{oil}}.$ If the oil drop does not carry sufficient kinetic energy to overcome

not carry sufficient kinetic energy to overcome all the relevant interfacial energies, it fails to separate from the water-air interface, and both oil and sheet spread out over the water surface.

In Fig. 2A, we show a phase diagram that summarizes the outcomes of experiments with circular sheets of thickness t=47 nm and varying We and W/R. The threshold We for successful wrapping (red line) increases with W/R. (Occasionally, even above the threshold We, the drop pinches off and separates from the interface but is pulled back onto the surface by transient fluid flows.) The final configurations above the threshold We, obtained for various values of W/R, are shown in Fig. 2B. As W/R increases, the sheet covers a larger portion of the drop's surface. For all the experiments shown in Fig. 2, we reproducibly

¹Department of Physics, University of Massachusetts, Amherst, MA 01003, USA. ²Polymer Science and Engineering Department, University of Massachusetts, Amherst, MA 01003, USA. ³Department of Physics, Syracuse University, Syracuse, NY 13244, USA. ⁴Materials Sciences Division, Lawrence Berkeley National Laboratory, Berkeley, CA 94720, USA. ⁵Beijing Advanced Innovation Center for Soft Matter Science and Engineering, Beijing University of Chemical Technology, Beijing 100029, China. ⁶Advanced Institute for Materials Research, Tohoku University, 2-1-1 Katehira, Aoba, Sendai 980-8577, Japan.

*Corresponding author. Email: menon@physics.umass.edu

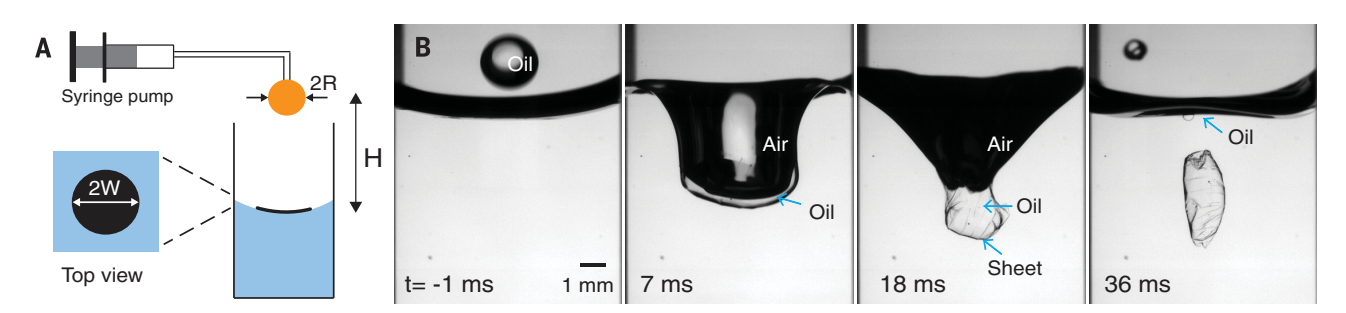


Fig. 1. Process of wrapping a splashing drop with a thin sheet. (A) Schematic of the experiment. (B) Sequence of events observed in a typical experiment where a fluorocarbon oil drop is wrapped with a polystyrene sheet. Here, W/R = 2.4, W = 400, and thickness t = 47 nm.

obtain the optimal 2-fold shape (reminiscent of an empanada) near complete wrapping ($W/R \cong 2.26$). This process rarely gets stuck in competing, near-optimal states (such as the 3-fold state) found in the quasistatic experiments (7). For larger W/R, the sheet has more area than is required to cover the droplet and forms crumpled, but closed, wrappings.

Bending energies of the wrapped state are expected to be negligible compared with interfa-

cial energies; this competition may be quantified by the bendability, a dimensionless number, given by (8): $\gamma W^2/B$, for a sheet of size W, Young's modulus E, Poisson ratio Λ , and bending stiffness $B\left(=\frac{Et^3}{12(1-\Lambda^2)}\right)$. Our experiments are conducted at high bendability (~10⁴ to 10^7) (6, 8, 11). The assumption that bending energy can be neglected is confirmed by experiments on films with a range of thicknesses (t = 46 to 372 nm) keeping W/R constant (Fig. 2C). There is no measured thickness dependence in the outcome. Neglecting bending energies in the sheet, we estimate a threshold We by considering the difference in sur-

face energies of the initial and final configura-

tions (see the supplementary text). This estimate

is an order of magnitude lower than the observed

threshold (see Fig. 2A). This estimate fails because it only considers the energies of the initial and final states and neglects the barrier presented by intermediate states as the oil drop pierces the water surface [unlike (5, 7)] to create a topologically distinct final state with a new set of interfaces. The sequence of images in Fig. 1 (see also movie S1) shows that the impact sets the water surface in motion, forming a crater that grows in size, reaches a maximum, and then collapses back to a flat interface. When the interface begins to rapidly relax back from the highly deformed shape, the oil at the interface collects into a drop, forms a neck, and pinches off to detach from the interface. This motivates the hypothesis that successful wrapping events can be understood as the pinch-off of a pendant drop. Moreover, in successful penetration events, a part of the oil drop is left behind at the interface, which is another characteristic of pinch-off.

To understand wrapping as a pinch-off of a pendant drop, we study droplet impact in the absence of a sheet. Although many studies have looked at the impact of a drop of liquid on a bath of identical or miscible liquid (12–15), few have considered immiscible liquids (10).

The oil in our experiments is denser than water, but a drop of small enough radius R placed gently at the surface will float because the force of surface tension ($F_{\gamma} \sim 2\pi R \gamma$, ignoring the geometry of the Neumann contact) exceeds the force of gravity ($F_g = \frac{4}{3}\pi R^3 \Delta \rho g$, where $\Delta \rho = \rho_{oil} - \rho_w$). Above a threshold size $R_0 = \sqrt{\frac{3}{2}} \ l_c$ set by the capillary length $\left(l_c = \sqrt{\frac{\gamma}{\Delta \rho g}}\right)$, gravity dominates the oilwater surface tension ($F_g > F_{\gamma}$), and the drop sinks and pinches off. However, a smaller drop can penetrate the surface if it has sufficient initial velocity (see Fig. 2A, W/R = 0). Figure 3A shows the time evolution of the height (y) of the

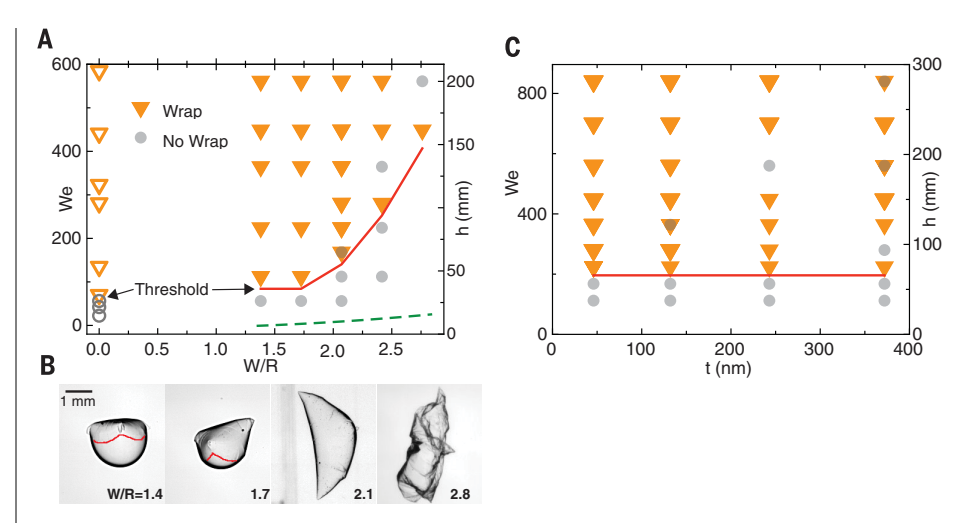


Fig. 2. Threshold for successful wrapping. (**A**) Data points indicate the outcome of the experiment as a function of We and W/R. The red curve shows the observed threshold for successful wrapping. The dashed green curve shows a naive threshold computed from the difference in the surface energies between the initial and the final states, assuming no loss of energy to the fluid. The open symbols represent experiments on a bare water surface without any sheets. (**B**) Examples of structures obtained for various W/R values. For clarity, boundaries of sheets (red curves) have been drawn by hand for W/R = 1.4 and 1.7. (**C**) The threshold W for successful wrapping shows no dependence on the thickness t. Here, W/R = 2.4. In some cases (gray circles above the threshold), a wrapping forms, but fluid recirculation in the cell brings it to the surface, causing it to unwrap.

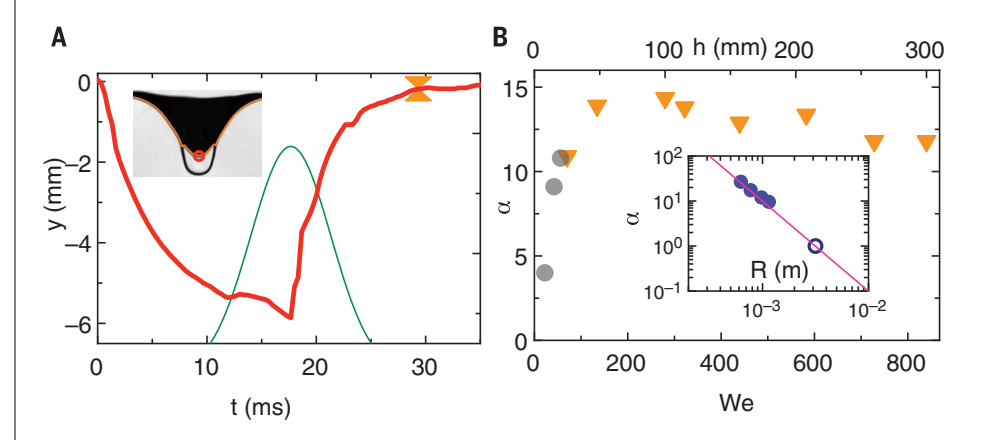


Fig. 3. Pinch-off dynamics in the absence of a sheet. (A) Time evolution (red curve) of the lowest point (red circle) of the air surface (orange curve in the inset) for We=320 in the absence of a sheet. The hourglass marker shows the instant when the pinch-off of the oil drop is complete. The oil-water interface (dark-light contrast) is also clearly visible. The acceleration α is computed with a Gaussian derivative filter (green curve). (B) The values of $\alpha = \frac{a+g}{g}$ obtained as a function of We (or h) for R=1.15 mm. Circles mark no penetration, triangles successful penetration. (Inset) The value of α at threshold for different drop sizes R. Filled circles represent splashing experiments, whereas the open circle represents a quasistatic experiment. The red line is the function $\alpha = \frac{3}{2} \left(\frac{l_c}{R}\right)^2 = \left(\frac{3}{2}\right) \left(\frac{\gamma}{g(\rho_0 - \rho_w)}\right) R^{-2}$.

lowest point on the interface after the impact of a drop of radius $R < R_0$. The water-air interface accelerates upward against gravity in the moments leading up to the detachment of the drop (indicated by the hourglass marker). In this dynamic version of pinch-off, the effective downward force on the drop is boosted by a factor $\alpha = \frac{a+g}{g}$, where

a is the upward acceleration of the interface measured in the lab frame. Our hypothesis is that the

threshold size for pinch-off is simply modified to $R_0 = \sqrt{\frac{3}{2\alpha}} \, l_c.$

To test this idea, we show in Fig. 3B the nondimensional acceleration α computed from the y(t) curves (see the supplementary text), in the absence of a sheet, as a function of release height (h) and We. The value of α initially increases with We but then saturates at approximately the threshold We required for successful penetration of the

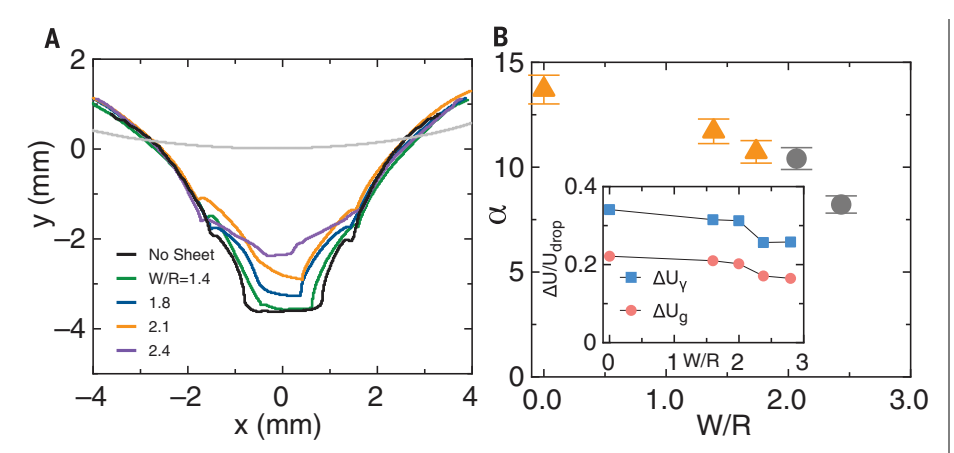


Fig. 4. Effect of the sheet on pinch-off dynamics. (A) Profiles of the air cavity 10 ms after impact for We = 112 and different W/R. The oil and sheet lie under the rough, central part of the profile and join the smooth air-water interface at the kink. The gray curve shows the air-water interface before the impact. (B) The nondimensional acceleration α as a function of W/R for We = 112. Triangles and circles represent wrap and no-wrap situations, respectively. The inset shows the change in surface and gravitational energies (see the supplementary text and fig. S3) computed at the parameter values of (A).

drop (orange triangles). The threshold depends on the size of the drop (R), because the two forces scale differently with the radius of the drop $(\sim R^3)$ and $\sim R$, respectively). The inset shows the

measured value of α at the threshold as a function of R. We also plot the result from the quasistatic experiment (i.e., $\alpha = 0$), where a drop is gently placed at the water surface and

its volume gradually increased until it becomes unstable and sinks. The predicted relationship $\left(\alpha = \frac{3}{2} \left(\frac{l_c}{R}\right)^2\right)$ describes all the data with no adjustable parameters (red curve in Fig. 3B). We emphasize, however, that this is far from a complete predictive understanding: α is a measured quantity that is controlled by the hydrodynamics of the impact, and its functional dependence on We is unknown.

The energy transfer from the drop during the impact is further modified by the elastic sheet (5, 16); the threshold We increases upon increasing the size of the sheet. For a given We, the interface deforms less for larger sheets, as shown by profiles of the air-water interface displayed in Fig. 4A and fig. S4. Correspondingly, the acceleration α decreases with increasing W/R as shown in Fig. 4B for We=112. Thus, at this fixed value of We, wrapping occurs for small W/R but fails at larger W/R (circles). Although the sheet is extremely flexible, it affects fluid dissipation, presumably by changing the boundary condition for fluid flow at the interface from being free in the case of an air-water interface to a no-slip condition when covered with the sheet. We notice from Fig. 2, A and C, that the threshold We as $t \rightarrow 0$ is different from the limit as $W/R \rightarrow 0$; that is, even an arbitrarily thin sheet modifies the dynamics of splashing.

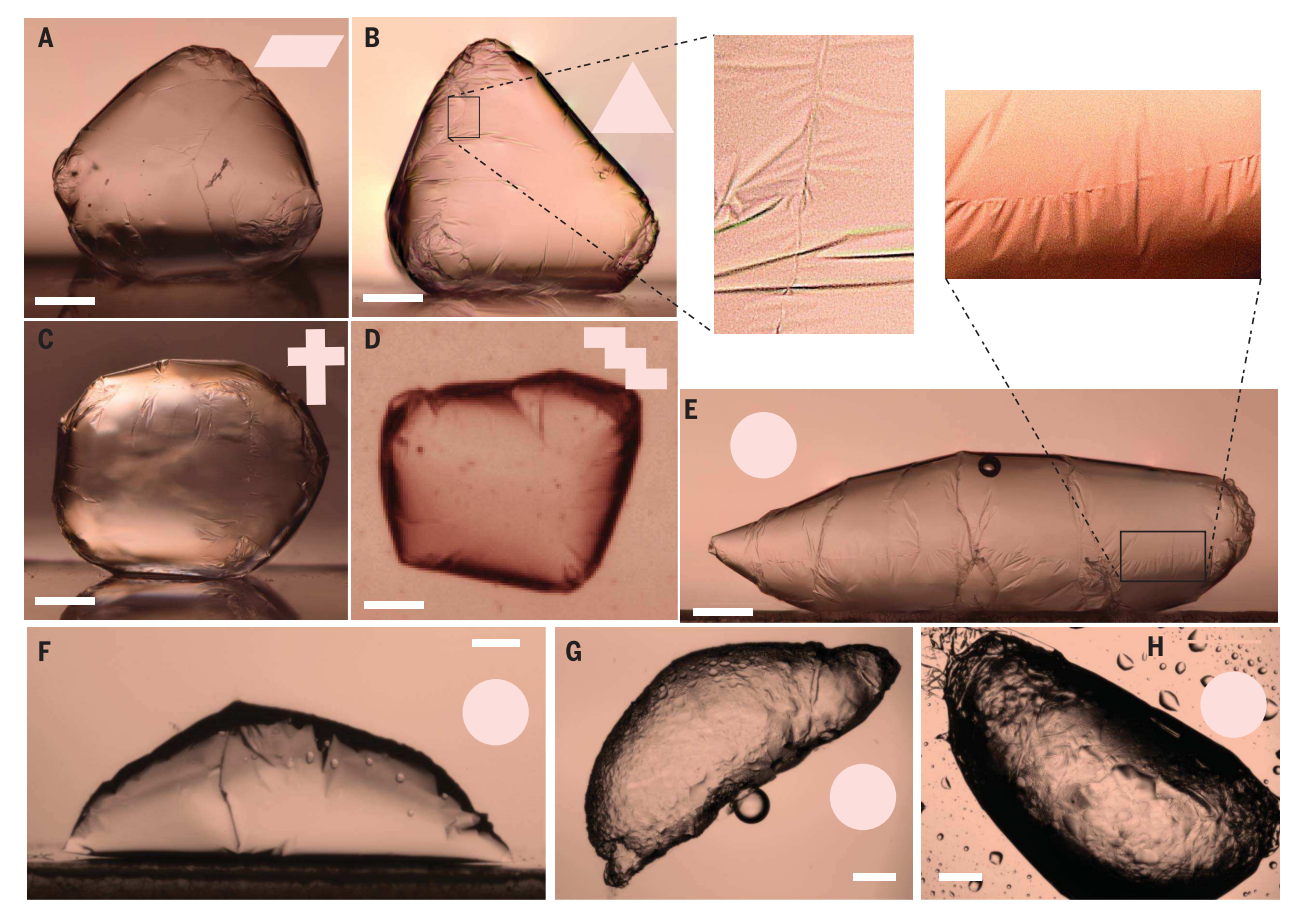


Fig. 5. Versatility of wrapping technique. (A to E) Different 3D shapes obtained from wrapping a drop of fluorinated oil inside water using sheets whose shapes are sketched in the insets. The quality of the seam is highlighted by the magnified sections of the images. (F) Mineral oil wrapped in an ethanol environment. (G) Water drop wrapped in a hexadecane environment. (H) Water drop extracted out in air from hexadecane. Scale bar, 0.5 mm.

Using the profiles shown in Fig. 4A and assuming axial symmetry, we compute the interfacial areas and, hence, the total surface and gravitational energies (see the supplementary text and fig. S3) 10 ms after impact for different values of W/R. The surface and gravitational energies decrease modestly with increasing W/R. Taken together, these account for a substantial fraction of the incoming kinetic energy of the drop.

We thus validate a picture of the underlying physics of droplet penetration as a pinch-off process driven by the large acceleration of the interface resulting from impact: We are able to correctly predict acceleration as a function of radius (Fig. 2B) and understand qualitatively the effect of the sheet in the splash. A solid sheet can profoundly affect the transfer of energy to the fluid, even if it is too thin to store elastic energy. Our data (Fig. 4B) more sharply pose a central question in the hydrodynamics of an immiscible splash; droplet penetration can be understood if the retraction acceleration α is determined in terms of initial kinetic energy We.

We illustrate the potential of impact wrapping by showing that the 3D shape of the wrapped drop can be tailored by designing the planar shape of the sheet. We have studied wrappings with sheets cut in 2D shapes inspired by the geometry of folding polyhedra (17). A tetrahedron can be cut open into a planar sheet in many different ways (18), known as the nets or unfoldings. Two of the simplest polygonal unfoldings of a tetrahedron (18) indeed yield a 3D shape close to a tetrahedron (Fig. 5, A and B). We also examined two different possible nets of a cube. The resulting wrappings are shown in Fig. 5, C and D. We emphasize that unlike in origami, no features need be scribed along the intended folds of the planar net (19, 20); the 3D shape is guided purely by a 2D contour. This is remarkable, as a planar shape like an equilateral triangle can be folded into many different closed 3D shapes (21), but a high-symmetry wrapping is selected during splashing. The wrappings are also robust under mechanical perturbations; a wrapped object can be deformed substantially and reform into the optimal shape, with the free edges having realigned (movie S4).

The quality of encapsulation achieved in wrapping 3D objects with 2D sheets depends crucially on how well the free edges are aligned together. Close examination of the seam achieved in these wrappings (Fig. 5, B and E) reveals that the edges of the sheet avoid both an overlap and an opening. The absence of an overlap suggests that there is no self-adhesion. Thus, this method of encapsulation is also reversible and can be opened to release the encapsulated liquid or can spontaneously reform after being distorted (see movie S4). This near-perfect seam is also an efficient barrier to diffusion and evaporation (as shown in figs. S5 and S6 and movie S5) and in this respect can be superior to particulate encapsulants.

In Fig. 5, F and G, we demonstrate the generality of the process with examples of hydrocarbon oil wrapped in an ethanol phase and of a water drop encapsulated in a hydrocarbon environment. In these situations, the sheet can also be functionalized to accommodate any chemical incompatibility of the fluid with the sheet. In Fig. 5G, for example, we use a bilayer sheet with an amorphous fluorocarbon polymer (Cytop) on the oil side of the interface and polystyrene on the aqueous side, because polystyrene is degraded by prolonged contact with the hydrocarbon oil. Finally, in Fig. 5H, we demonstrate that the wrapped object may be extracted out of the liquid-liquid interface where it was created, provided that the surface energy of this interface is relatively low. Thus, the versatility and robustness of impact wrapping indicates the possibility of application in many settings for many pairs of liquids-e.g., as containers for chemical reactions, targeted delivery of tiny liquid cargo, or separation and isolation of unwanted liquid phases. Here, we use bilayer films to achieve chemical compatibility, but a large class of scalable techniques can be exploited to make polymer films with designed chemical functionality, optical qualities, or controlled permeability.

REFERENCES AND NOTES

- 1. B. P. Binks, T. S. Horozov, Colloidal Particles at Liquid Interfaces (Cambridge Univ. Press, 2006)
- M. Cui, T. Emrick, T. P. Russell, Science 342, 460-463 (2013).
- M. Abkarian, S. Protière, J. M. Aristoff, H. A. Stone, Nat. Commun. 4. 1895 (2013).
- 4. C. Py et al., Phys. Rev. Lett. 98, 156103 (2007).
- 5. A. Antkowiak, B. Audoly, C. Josserand, S. Neukirch, M. Rivetti, Proc. Natl. Acad. Sci. U.S.A. 108, 10400-10404 (2011).
- H. King, R. D. Schroll, B. Davidovitch, N. Menon, Proc. Natl. Acad. Sci. U.S.A. 109, 9716-9720 (2012).
- J. D. Paulsen et al., Nat. Mater. 14, 1206-1209 (2015).
- 8. B. Davidovitch, R. D. Schroll, D. Vella, M. Adda-Bedia, E. A. Cerda, Proc. Natl. Acad. Sci. U.S.A. 108, 18227-18232 (2011).
- Materials and methods are available as supplementary materials
- 10. H. Lhuissier, C. Sun, A. Prosperetti, D. Lohse, Phys. Rev. Lett. 110. 264503 (2013).
- 11. R. D. Schroll et al., Phys. Rev. Lett. 111, 014301 (2013)
- 12. W. C. Macklin, G. J. Metaxas, J. Appl. Phys. 47, 3963-3970 (1976).
- 13. A. I. Fedorchenko, A.-B. Wang, Phys. Fluids 16, 1349-1365 (2004).
- 14. L. J. Leng, J. Fluid Mech. 427, 73-105 (2001).
- 15. Y. K. Cai. Exp. Fluids 7, 388-394 (1989).
- 16. R. E. Pepper, L. Courbin, H. A. Stone, *Phys. Fluids* **20**, 082103 (2008).
- 17. E. D. Demaine, J. O'Rourke, Geometric Folding Algorithms (Cambridge Univ. Press, Cambridge, 2007).
- 18. J. Akiyama, K. Hirata, M. Kobayashi, G. Nakamura, Comput. Geom. 34, 2-10 (2006).
- 19. A. Terfort, N. Bowden, G. M. Whitesides, Nature 386, 162-164 (1997).
- 20. D. Gracias, V. Kavthekar, J. Love, K. Paul, G. Whitesides, Adv. Mater. 14, 235-238 (2002).
- 21. J. Akiyama, G. Nakamura, Combinatorial Geometry Graph Theory 3330, 34-43 (2005).

ACKNOWLEDGMENTS

We acknowledge financial support from the W. M. Keck Foundation, NSF-DMR 1506750 (N.M.), and NSF-DMR-CAREER-1654102 (J.D.P.). We also acknowledge valuable guidance from J. Chang in making thin films. Raw data supporting the results presented in the paper and the supplementary materials can be obtained by requesting them from the corresponding author.

SUPPLEMENTARY MATERIALS

www.sciencemag.org/content/359/6377/775/suppl/DC1 Materials and Methods Supplementary Text Figs. S1 to S6 Movies S1 to S5 Reference (22)

16 June 2017; accepted 13 December 2017 10.1126/science.aao1290



Wrapping with a splash: High-speed encapsulation with ultrathin sheets

Deepak Kumar, Joseph D. Paulsen, Thomas P. Russell and Narayanan Menon

Science **359** (6377), 775-778. DOI: 10.1126/science.aao1290

It's a wrap

Whether an object has a regular or irregular shape, wrapping it with a thin film can be challenging. Kumar *et al.* released droplets of oil above thin polymer sheets floating on water (see the Perspective by Amstad). With sufficient impact force, the polymer wrapped around the droplet with near perfect seams. The shape of the resulting enclosed drop depended on the shape of the sheet initially placed at the air-liquid interphase.

Science, this issue p. 775; see also p. 743

ARTICLE TOOLS http://science.sciencemag.org/content/359/6377/775

SUPPLEMENTARY http://science.sciencemag.org/content/suppl/2018/02/14/359.6377.775.DC1 MATERIALS

RELATED http://science.sciencemag.org/content/sci/359/6377/743.full

REFERENCES This article cites 18 articles, 4 of which you can access for free

http://science.sciencemag.org/content/359/6377/775#BIBL

PERMISSIONS http://www.sciencemag.org/help/reprints-and-permissions

Use of this article is subject to the Terms of Service